



PHYSICS AND ENGINEERING PHYSICS

# E region echo velocity and $E \times B$ as inferred from Stokkseyri observations

J. D. Gorin and A. V. Koustov

Institute of **S**pace and **A**tmospheric **S**tudies

# Outline:

1. Long introduction

2. Stokkseiry data:

Observations along ExB and away from it

3. Conclusions

# Syowa East and CRL 50-MHz radar concurrent observations (Koustov et al., 2001)

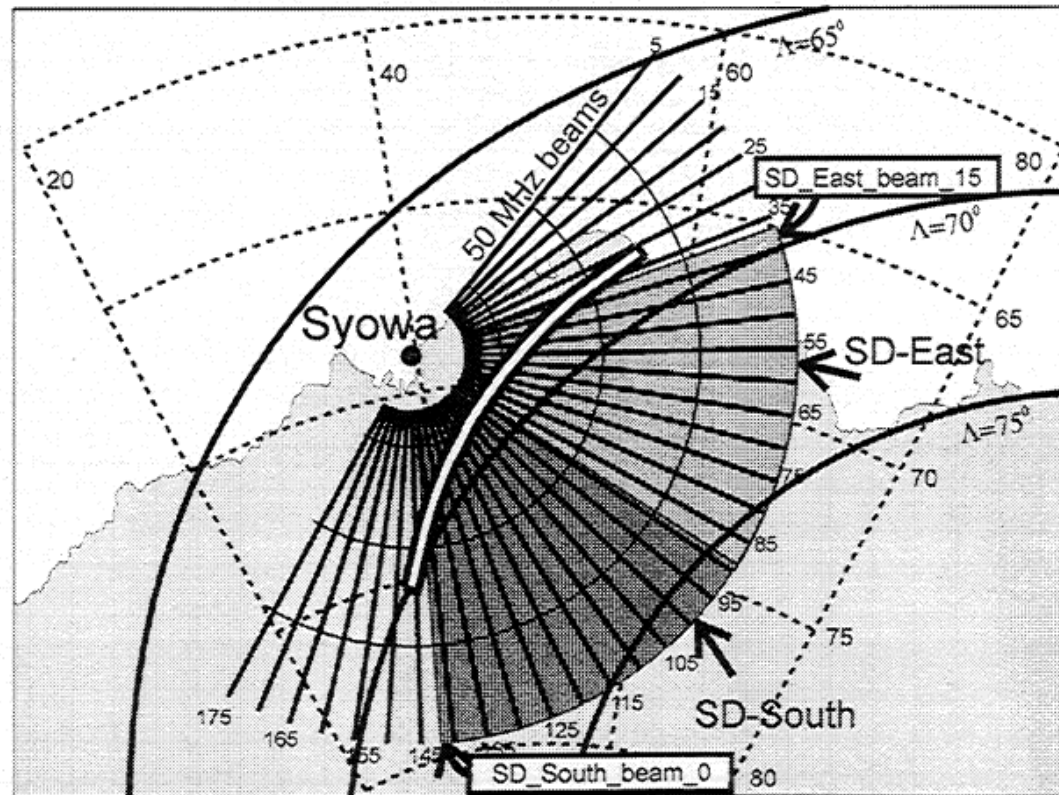
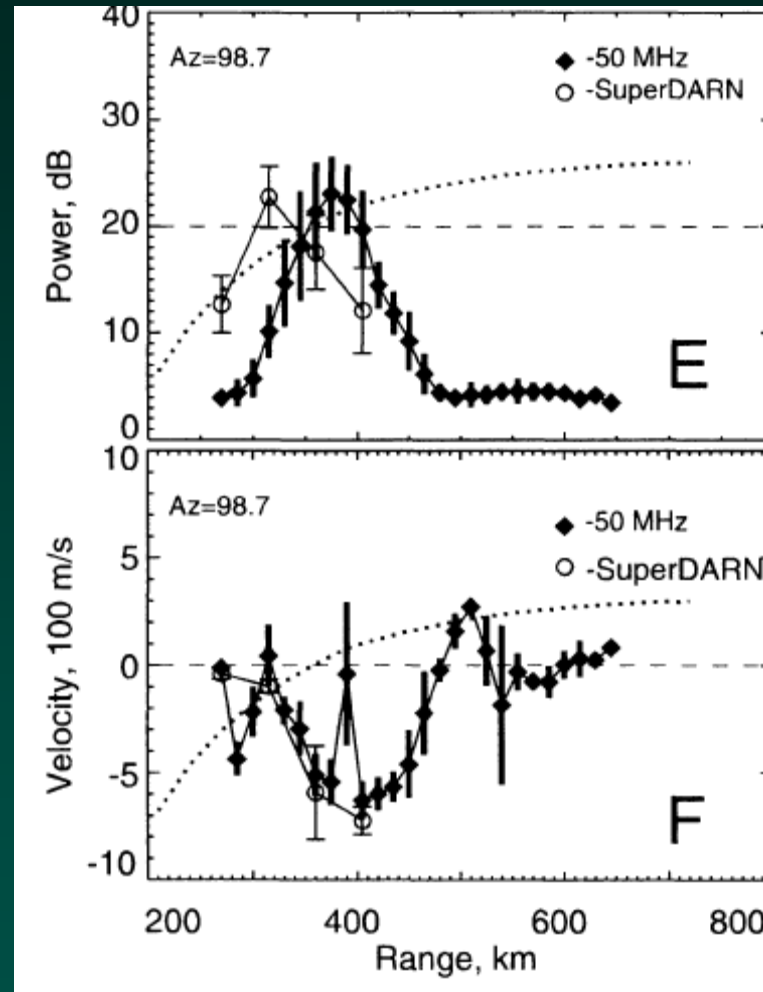


**Figure 1.** Viewing zones of Syowa Super Dual Auroral Radar Network (SuperDARN) HF radars (East and South) and the Communications Research Laboratory (CRL) 50-MHz radar. Also shown are Polar Anglo-American Coordinate System (PACE) lines of equal magnetic latitudes  $\Lambda=65^\circ$ ,  $\Lambda=70^\circ$ , and  $\Lambda=75^\circ$ . Heavy white curve is the zero off-perpendicular angle line (without consideration of ionospheric refraction).

**Beams 0-5 are almost along the ExB flow. There are 50-MHz beams in about the same directions. Aspect conditions are good.**

Quite often, HF velocity is very close to the VHF velocity. This happens in a number of radar cells.



Notice that HF velocity magnitudes are up to 700 m/s. So, high velocity E region echoes do occur. This happens when HF radio waves “penetrate” deep inside the layer

Occasionally,  
however, the HF  
velocity is MUCH  
LESS than the VHF  
velocity  
(Makarevich et al.,  
2003)

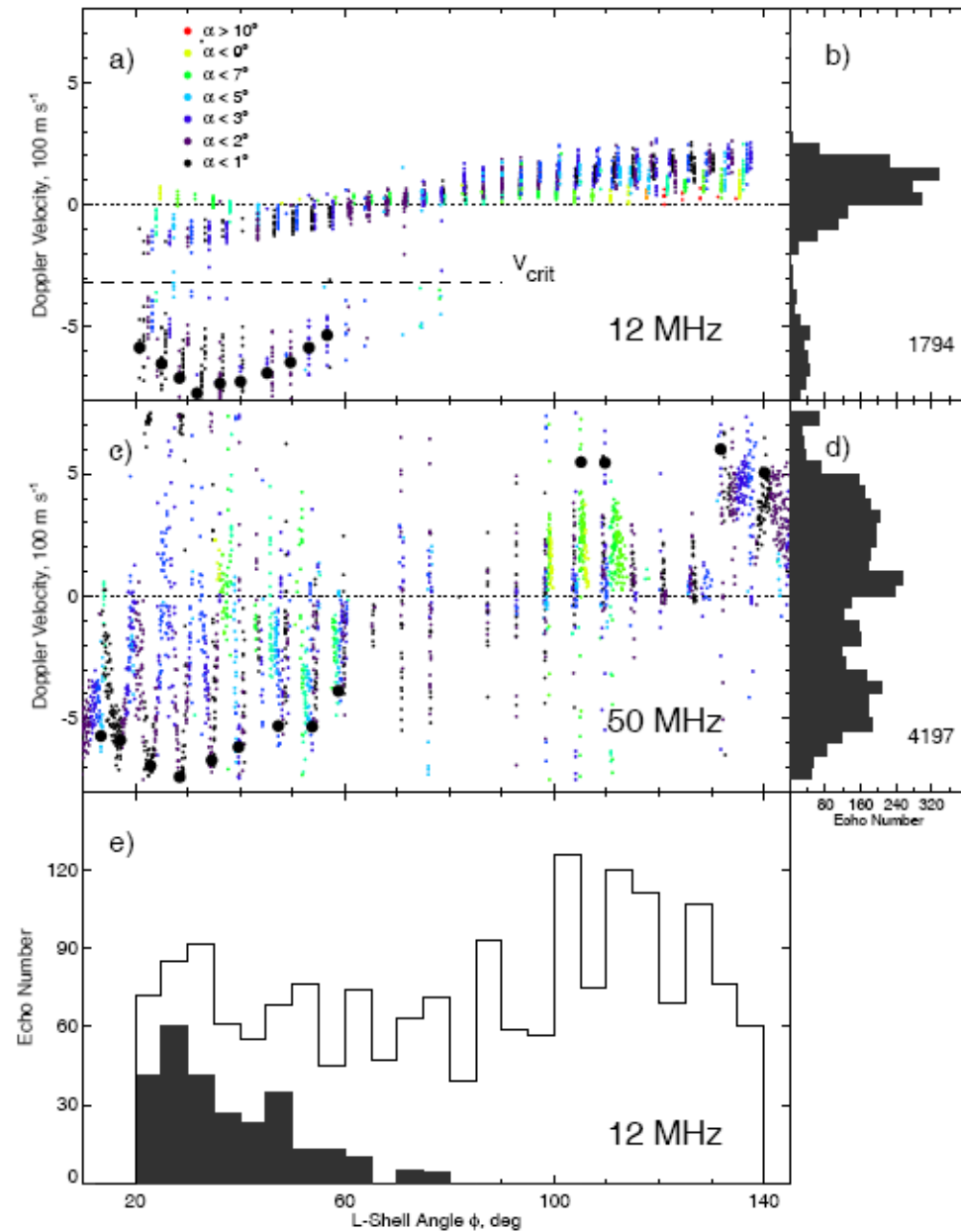
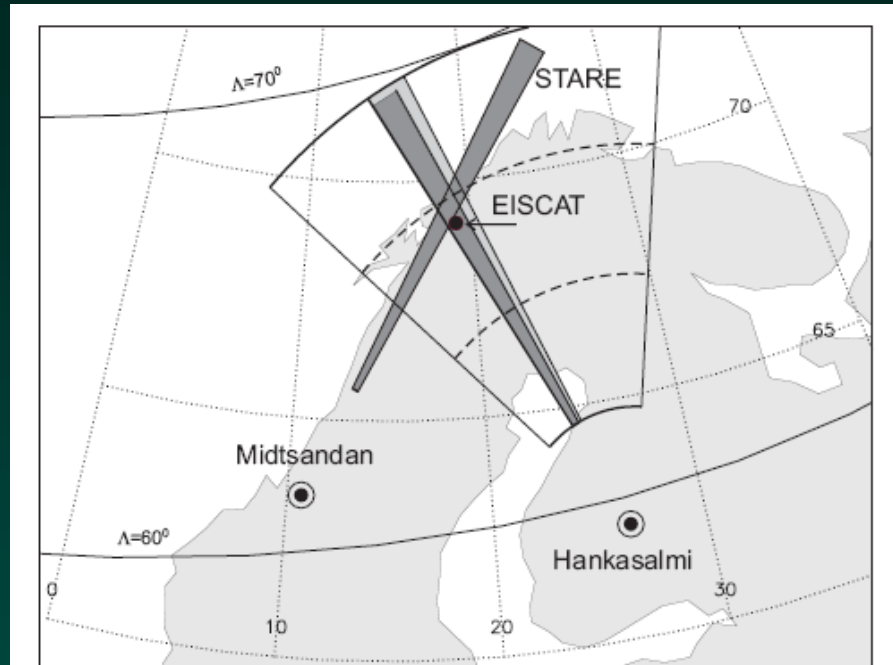


Figure 5.11: Doppler velocity versus  $L$ -shell angle at (a) 12 and (c) 50 MHz for March 17, 1997, 0100-0130 UT. Right panels are histograms of velocity distribution for (b) 12- and (d) 50-MHz radars. Panel (e) is the histogram of number of echoes (in  $5^\circ$ -wide bins) versus the  $L$ -shell angle at 12 MHz.

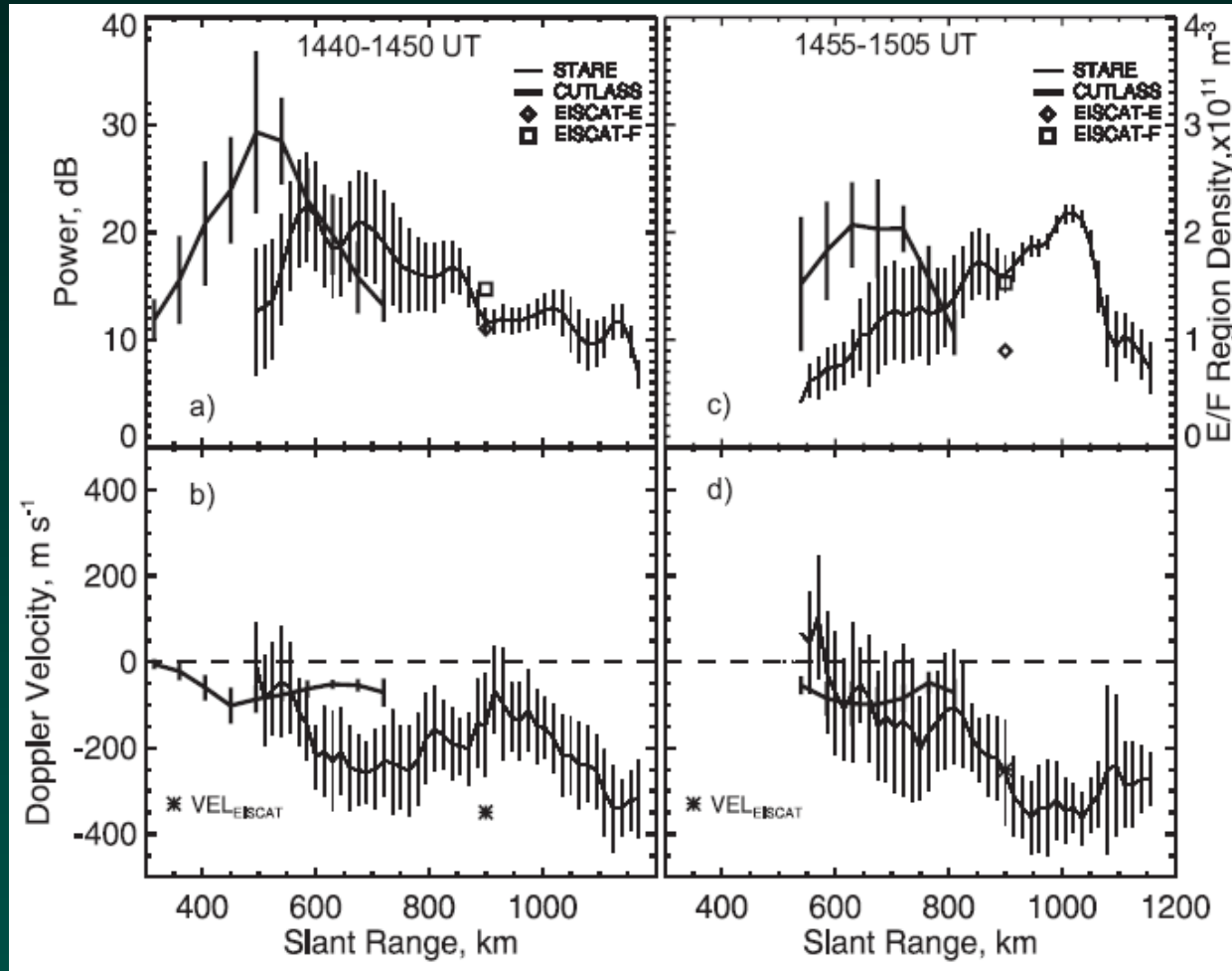
# Hankasalmi HF and STARE VHF (150-MHz) radar concurrent observations (Koustov et al., 2002)



**Fig. 1.** Field-of-view of the Hankasalmi CUTLASS HF radar for ranges between 300 and 1200 km at the height of 110 km. Dashed lines are slant ranges of 600 and 900 km. The lightly shaded sector is the location of the CUTLASS beam 5. The darker beam-like sectors are the location of the Finland STARE radar beam 3 and the Norway STARE radar beam 4. The solid dot denotes the area where ionospheric parameters were monitored by the EISCAT incoherent scatter radar. Also shown are PACE lines of equal magnetic latitudes  $\Lambda = 60^\circ$  and  $\Lambda = 70^\circ$ .

**There are several overlapping beams. Aspect conditions are good.**

Quite often, HF velocity is much LESS than the VHF velocity. This happens in a number of radar cells.



Notice that VHF velocity magnitudes are small due to aspect angle attenuation. The ExB component along the beams is ~300 m/s, while the total ExB > 1000 m/s.

# Some recent accomplishments, I:

Annales Geophysicae (2004) 22: 1177–1185  
SRef-ID: 1432-0576/ag/2004-22-1177  
© European Geosciences Union 2004



## Simultaneous HF measurements of E- and F-region Doppler velocities at large flow angles

R. A. Makarevitch<sup>1</sup>, F. Honary<sup>1</sup>, and A. V. Koustov<sup>2</sup>

<sup>1</sup>Department of Communication Systems, Lancaster University, Lancaster, LA1 4YR, UK

<sup>2</sup>Institute of Space and Atmospheric Sciences, University of Saskatchewan, 116 Science Place, Saskatoon, SK, S7N 5E2, Canada

Received: 3 June 2003 – Revised: 30 October 2003 – Accepted: 5 November 2003 – Published: 2 April 2004

University of  
Saskatchewan





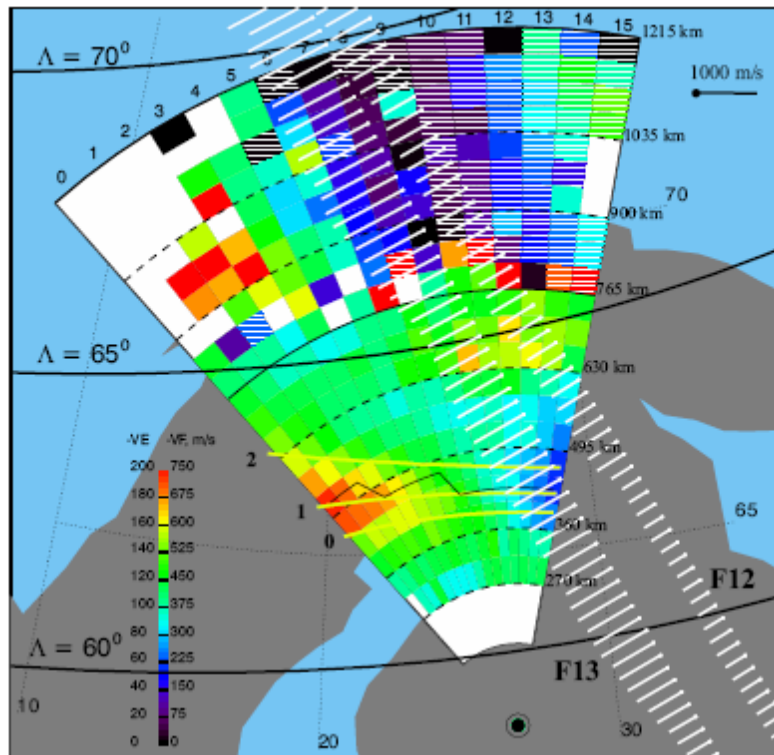


**Fig. 1.** Field of view plot of the averaged Doppler velocity observed by the CUTLASS Finland radar during the interval 14:40–14:50 UT on 31 March 2000. Each radar cell is color coded according to the color bar shown in the left bottom part of the diagram. The color scheme for  $r=180-765$  km ( $r=765-1215$  km) is indicated by the digits to the left (right) of the color bar. The echoes in cells filled by the horizontal lines have, on average, positive velocities corresponding to the color of the line. Also shown are slant range marks (dashed circular curves) and PACE lines of equal magnetic latitudes  $\Lambda=60^\circ$ ,  $65^\circ$ , and  $70^\circ$  (solid thick curves). Thick yellow curves 0–2 denote the off-perpendicular (aspect) angle  $\alpha=0^\circ$  (see text for details). Thin ragged solid black line shows the location of the average power maxima along each radar beam. Two DMSP passes (F13: 14:43–14:48 UT and F12: 17:05–17:10 UT) with the measured perpendicular ion velocities are indicated by white vectors. The scale for the ion velocities is shown in the top right corner of the diagram.

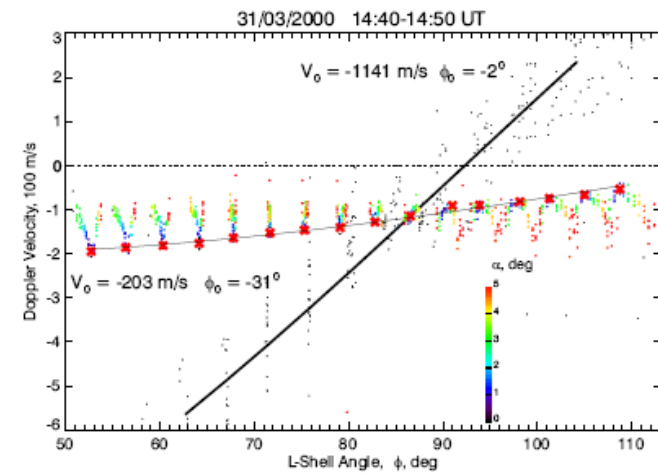


**Fig. 3.** Scatter plot of the Doppler velocity versus  $L$ -shell angle  $\phi$  for 31 March 2000, 14:40–14:50 UT. The points corresponding to E-region scatter are color coded in aspect angle  $\alpha$ , as indicated in the bottom right part of the diagram. The red crosses are maxima/minima of the averaged velocity along radar beams, as described in the text. The F-region velocities are shown by black points. The solid thin (thick) line represents the best fit,  $V_0 \cos(\phi + \phi_0)$ , to red crosses (all black points).

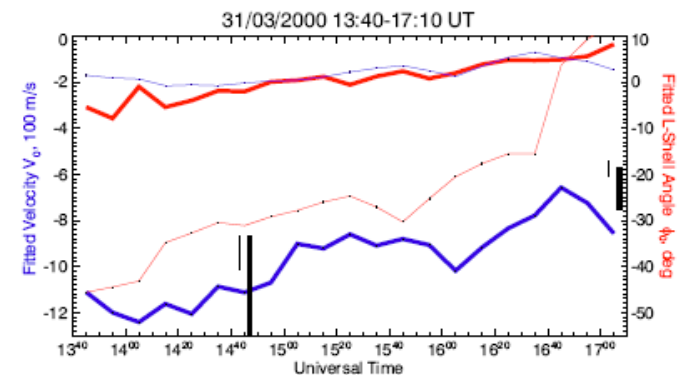


**Fig. 4.** Time variation of the fitted velocity  $V_0$  (blue) and  $L$ -shell angle  $\phi_0$  (red) during the considered period. The scale for the fitted velocity ( $L$ -shell angle) is shown on the left (right) axis. Thin (thick) line represents the results of fitting for E- (F-) region. Vertical thin (thick) black lines show the span (minimum to maximum) of the DMSP measurements of the ion drift in the latitudes corresponding to E- (F-) region for the two passes over the FoV shown in Fig. 1.

# Some recent accomplishments, II:

Annales Geophysicae (2005) 23: 1–9  
SRef-ID: 1432-0576/ag/2005-23-1  
© European Geosciences Union 2005



## On the relationship between the velocity of E-region HF echoes and $E \times B$ plasma drift

A. V. Koustov<sup>1</sup>, D. W. Danskin<sup>2</sup>, R. A. Makarevitch<sup>3</sup>, and J. D. Gorin<sup>1</sup>

<sup>1</sup>Institute of Space and Atmospheric Studies, University of Saskatchewan, 116 Science Place, Saskatoon, S7N 5E2 Canada

<sup>2</sup>Geological Survey of Canada, Geomagnetic Laboratory, 7 Observatory Cres., Ottawa, K1A 0Y3 Canada

<sup>3</sup>Department of Communication Systems, Lancaster University, Lancaster, LA1 4YR, UK

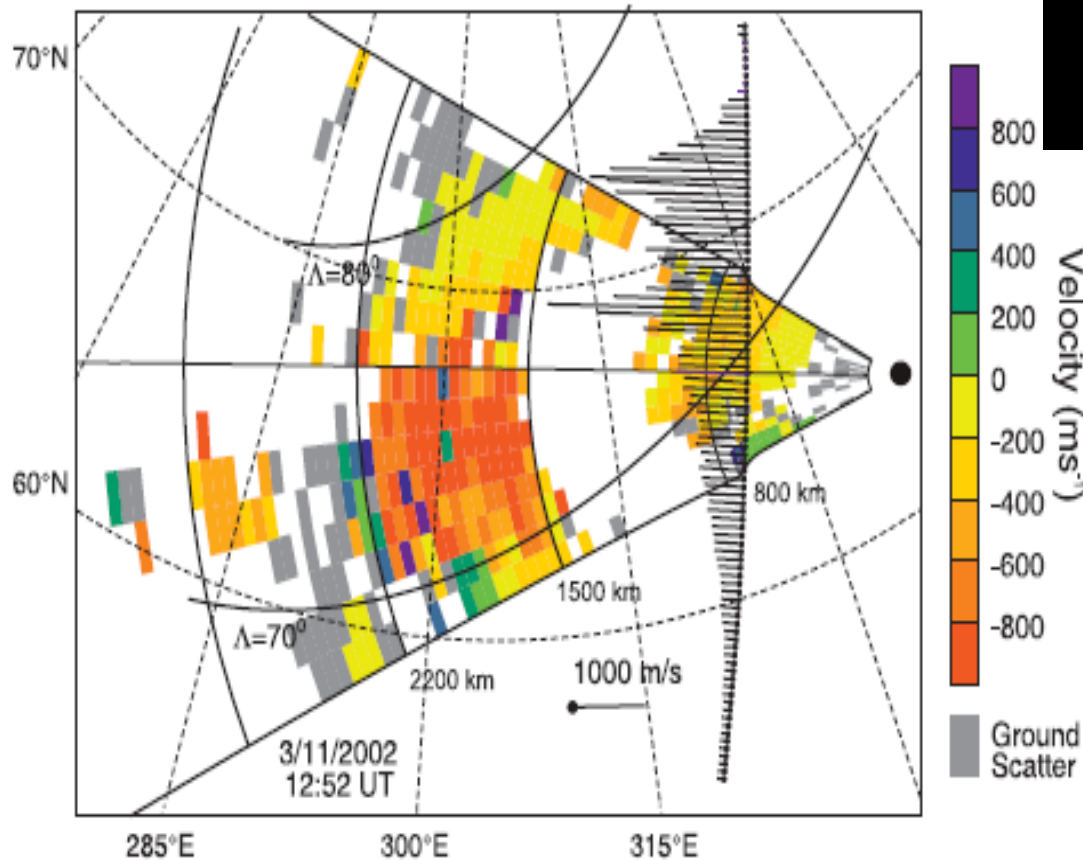
Received: 26 April 2004 – Revised: 18 October 2004 – Accepted: 21 October 2004 – Published:

University of  
Saskatchewan



# Combination of the Stokkseiry HF radar and DMSP in situ data

- Flows are predominantly along L shells so that observations are mostly along ExB





# Summary on previous results:

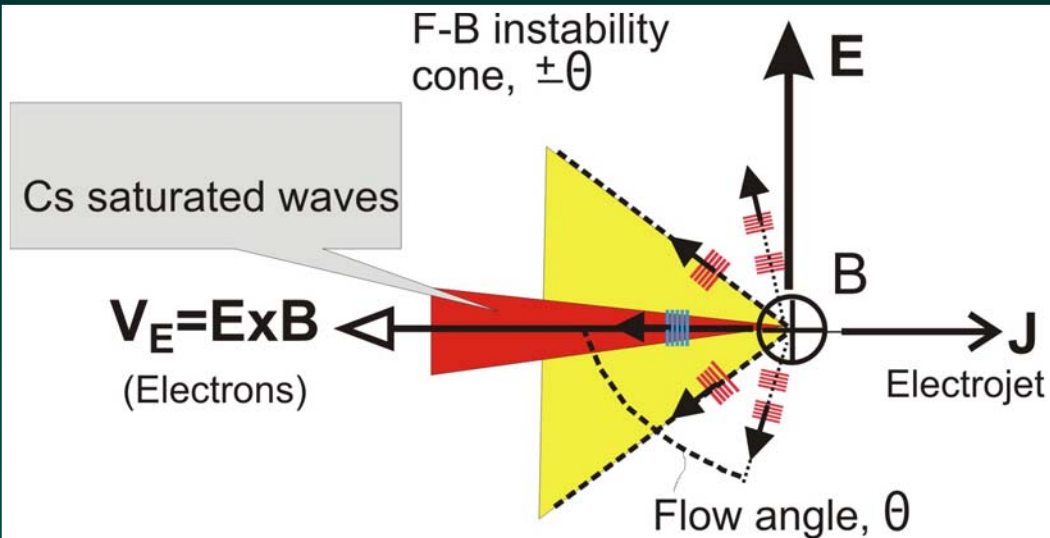
Quite often the velocity of E region echoes is well below the  $E \times B$ . This happens for sure for observations at large flow angles.

# Questions for investigation:

Does this happen for observations along the  $E \times B$ ? I mean on a more significant basis than the Antarctica comparison. And what do we have for these directions anyway? We certainly expect the Cs saturation phenomenon that has been discussed in a number of studies.

Something new in the field:

Bahcivan et al. (2005) hypothesized that  $C_s$  saturated irregularities exist only almost strictly along the flow while the velocity is  $C_s \cos \theta$  at all other directions (the “ $C_s$  hypothesis”).



Cs saturated FB waves  
along  $E \times B$

$$V_{ph} = C_S$$

All other directions:

$$V_{ph} = C_S \cos \theta$$

**Finally, something new that has been  
done at the U of S**

University of  
Saskatchewan





# Stokkseyri geometry

- Southernmost beams of Stokkseyri are roughly L-shell aligned
- The evening sector flow is mostly along L shells

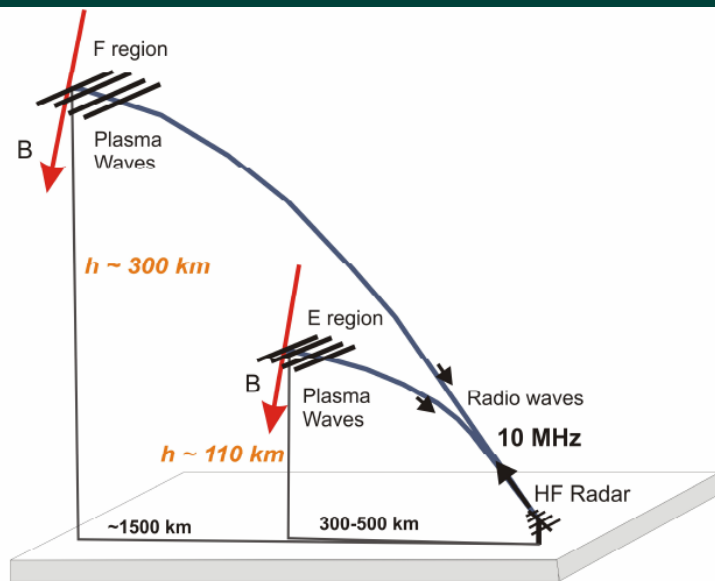
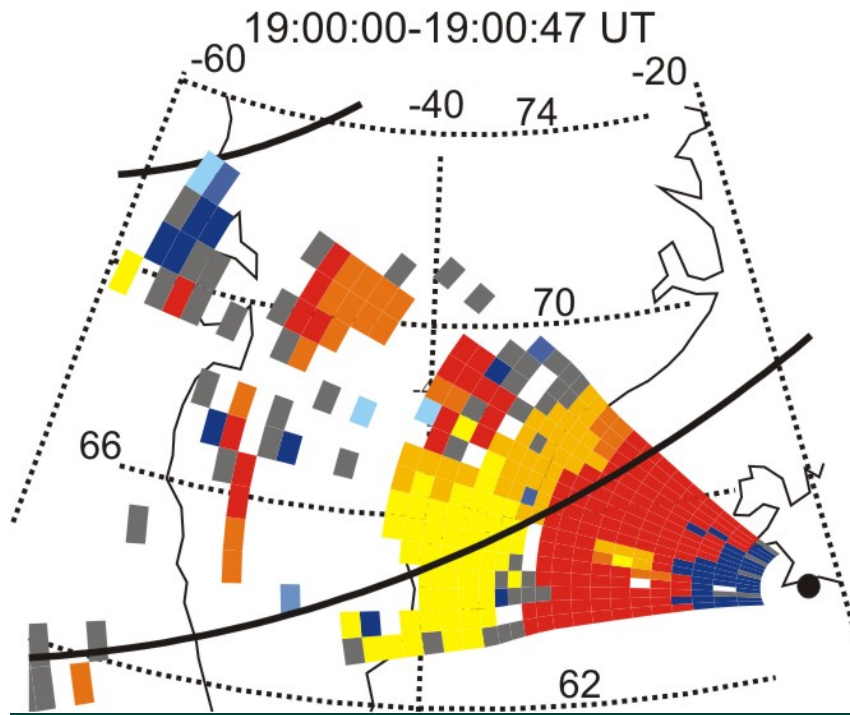


Figure 2.5: Geometry of simultaneous detection direct scatter from E and F regions using SuperDARN HF radar (not to scale).

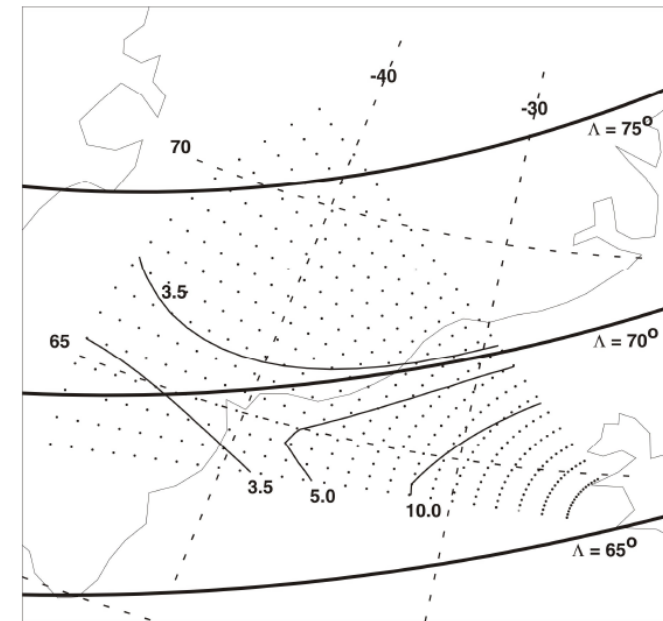


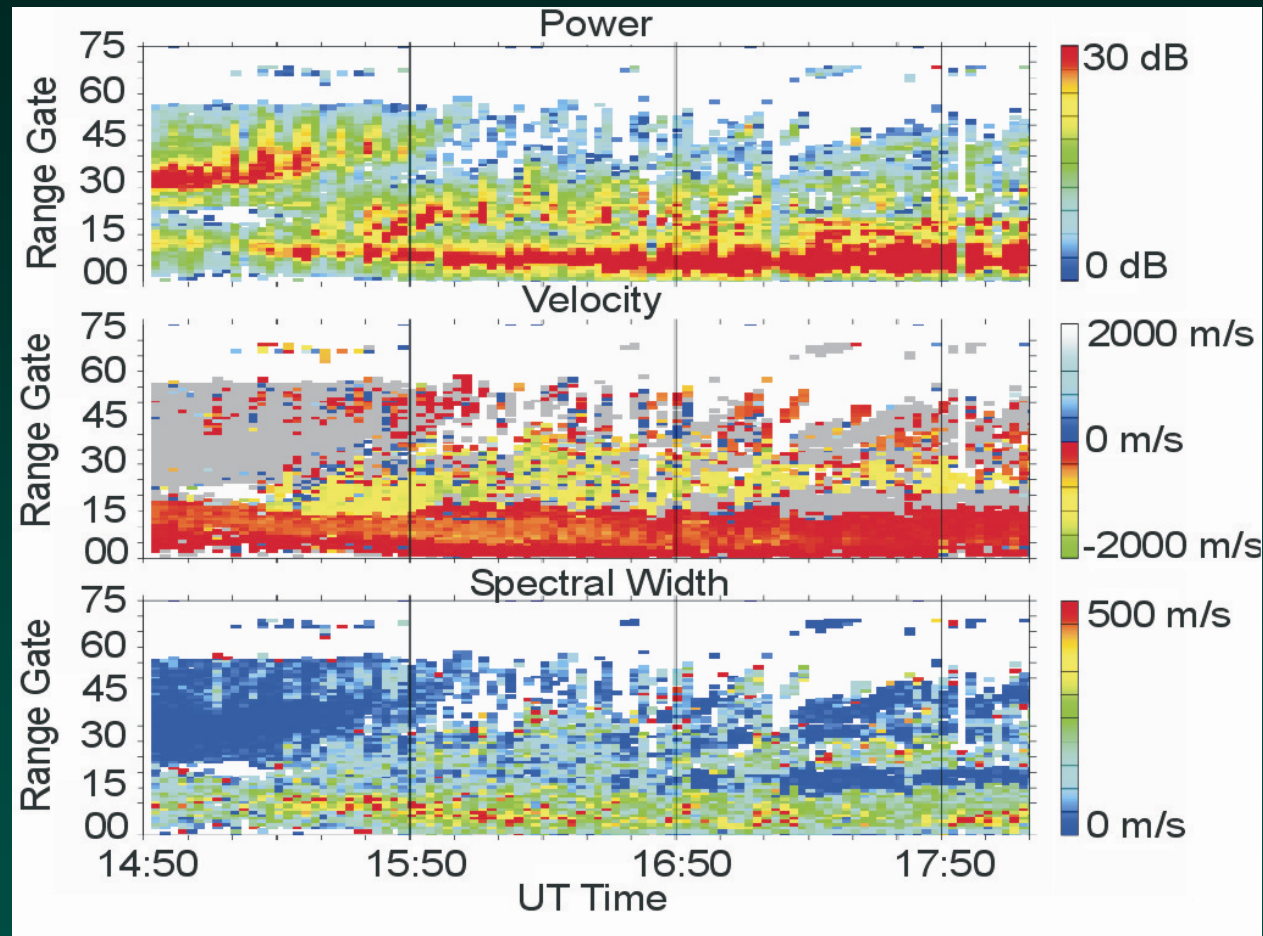
Figure 2.7: The field-of-view of the Stokkseyri SuperDARN radar for ranges 180 – 1260 km. Each dot represents the location of the beginning of a radar cell. A height of 110 km is assumed. The thin lines are the zero aspect angle lines for the shown peak electron densities (shown in units of  $10^{10} \text{ m}^{-3}$ ) at 110 km for a radar frequency of 12 MHz. The thick lines are the AACGM magnetic latitudes (from *Koustov et al., 2005*).



# Steps in work

- >30 events ranging in duration from ~30 min to several hours were considered
- Assessment for beams 0-2, roughly along the flow
- Assessment for all beams/all directions

# HF Velocity close to Cs (beam 1)



- Events with co-existing long-lived E and F region echoes along the southernmost beams of the Stokseyri SuperDARN radar are selected
- F-region echo velocity is used to estimate  $E \times B$  drifts in the E region

# Range profiles

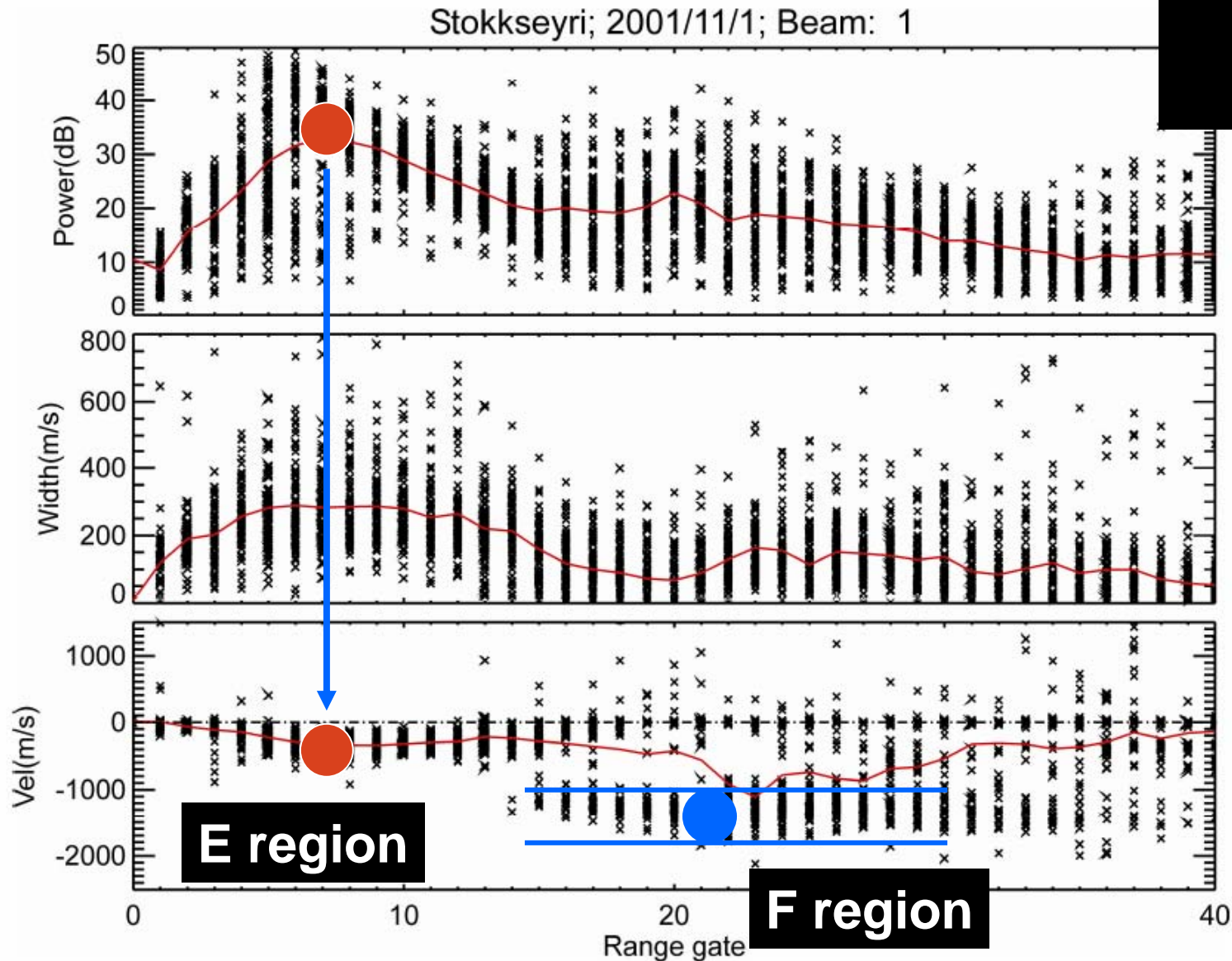


Figure 4.2: Echo power, spectral width and velocity recorded by the Stokkseyri radar for the entire event interval of 1 November 2001 in range gates 0 – 40. The red curve represent the average value of respective parameter at various range gates.

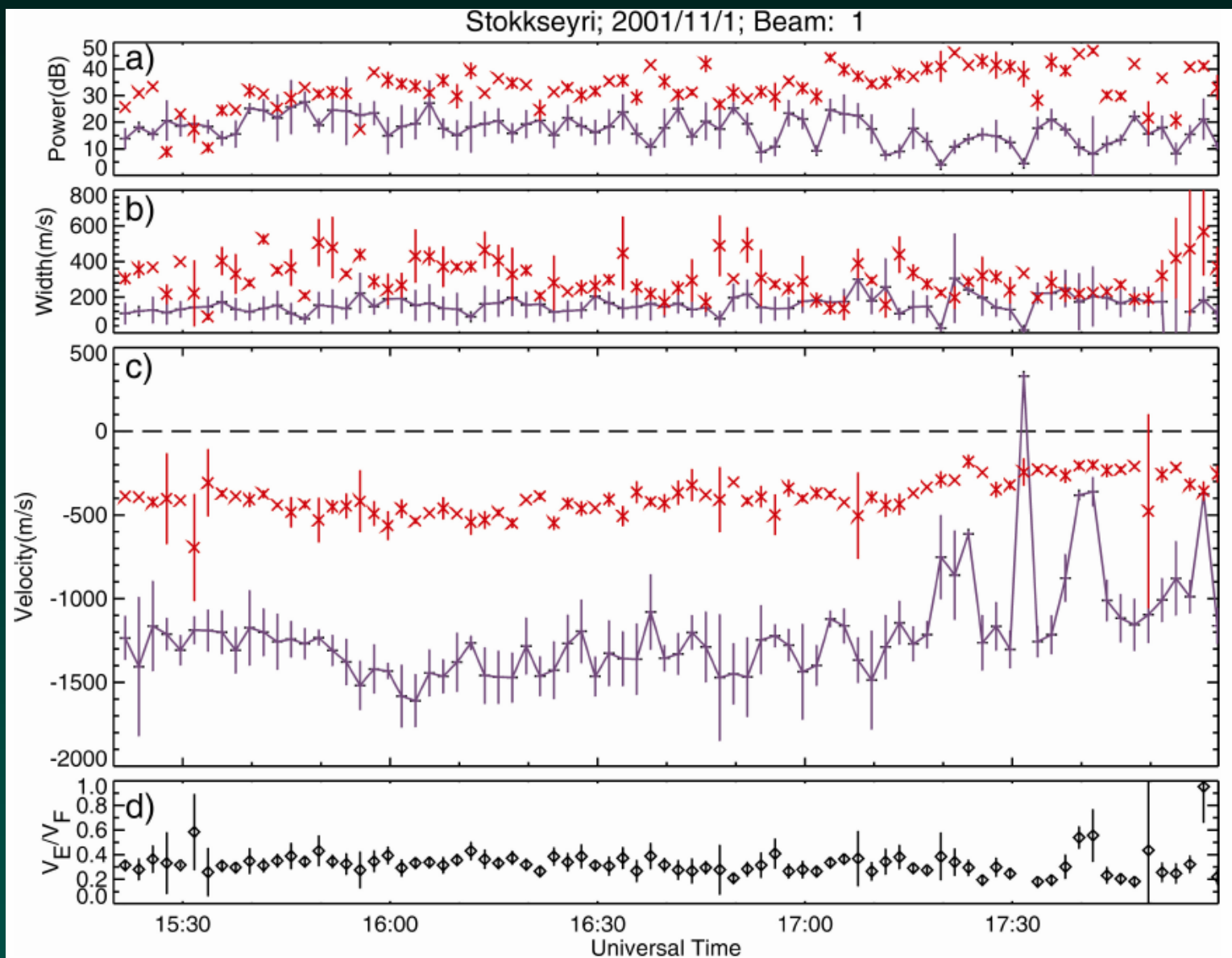
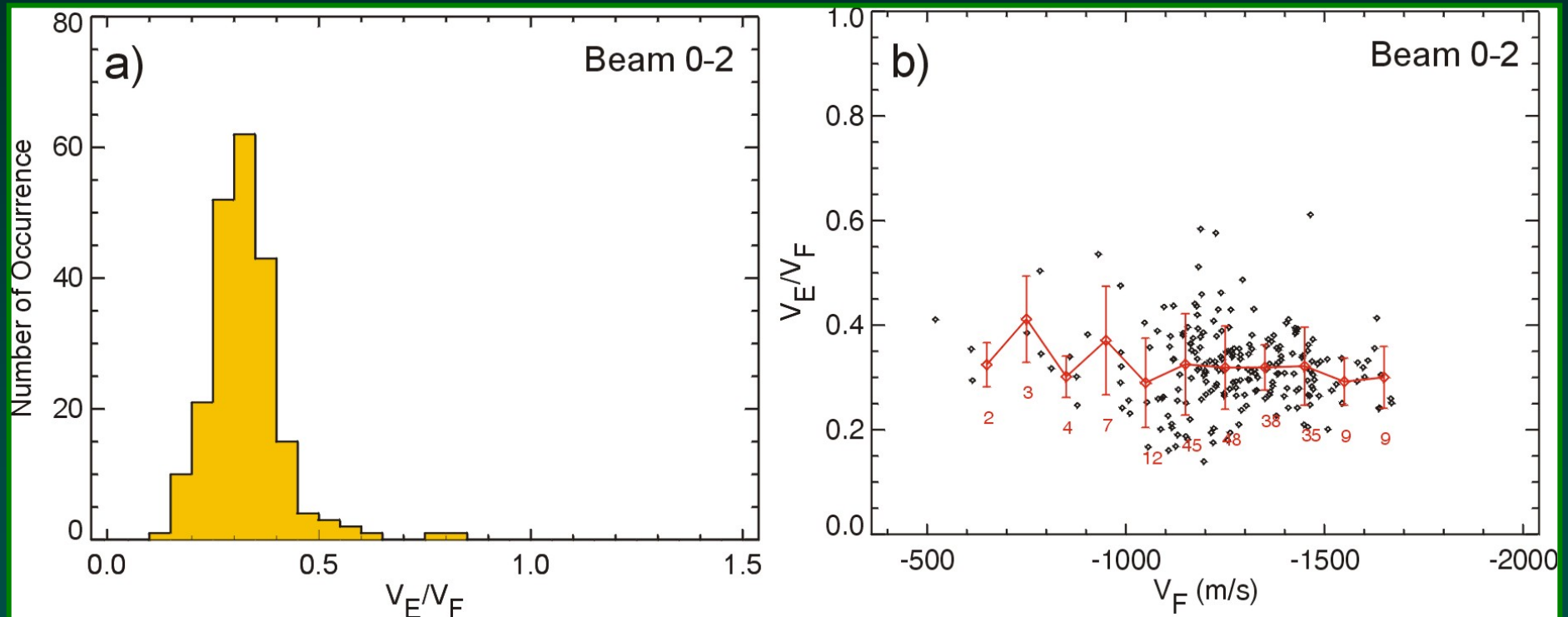


Figure 4.3: Temporal variations of (a) the averaged echo power, (b) spectral width and (c) velocity for the E-region and F-region echoes. Panel (d) shows the velocity ratio  $R = V_E/V_F$ . Red crosses represent the E-region parameters, plus signs connected by the lines represent F-region parameters and the diamonds are the ratio of the E-region velocity to the F-region velocity.

# High Velocity E region echoes, 1 Nov 2001 event

## Approach 1: One direction comparison, beams 0-2



The overall average ratio  $R = V_{HF} / V_{ExB}$  is 0.35 and decreases slowly with increasing **ExB** magnitude



# Approach 2: Flow Angle Variation

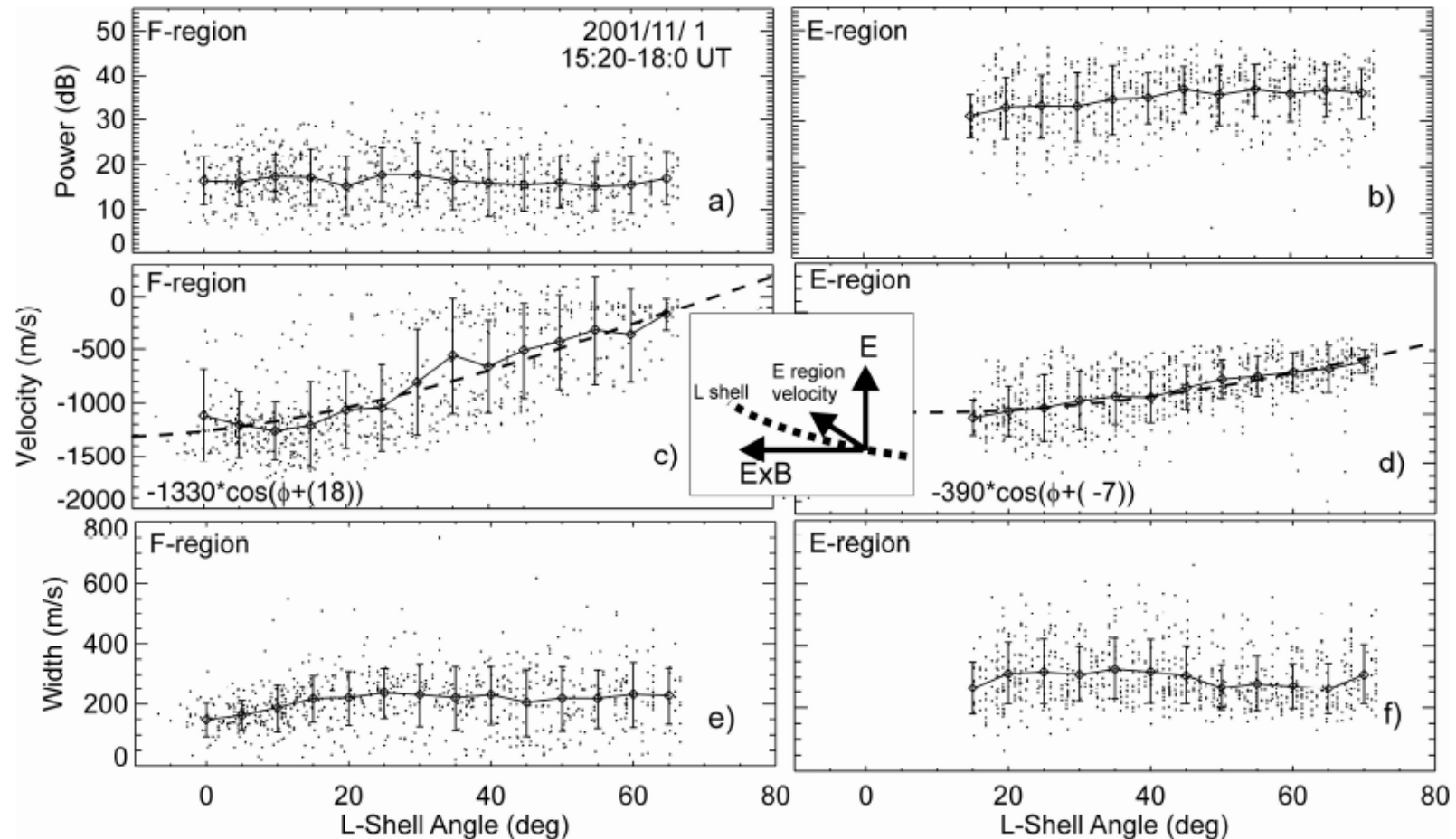
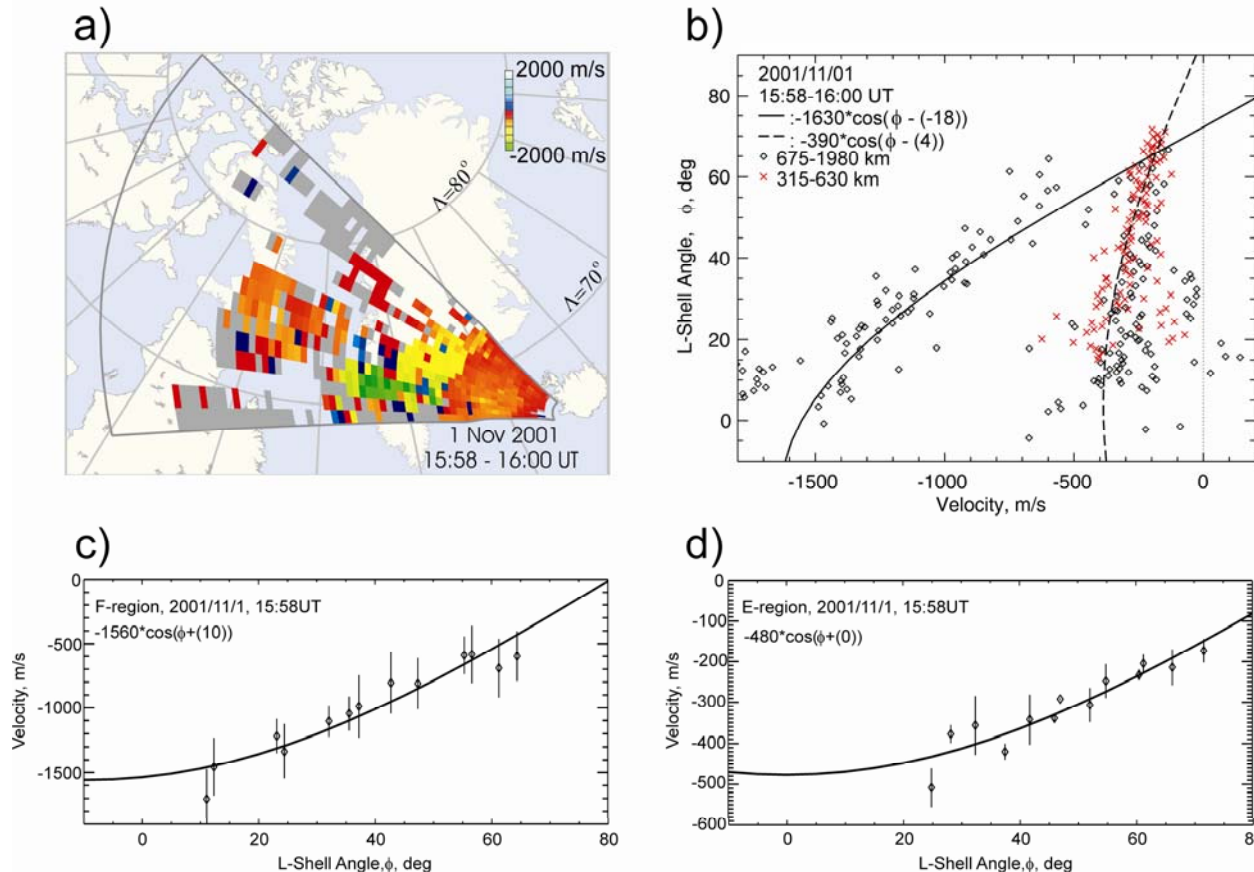


Figure 4.6: Scatter plot of measured echo power, velocity and spectral width for F-region and E-region echoes versus the L-shell angle. Data trends are illustrated by averaging (solid lines) and by fitting to a cosine function (dashed lines). The insert between panels (c) and (d) shows the directions of the E-region velocity and the  $\mathbf{E} \times \mathbf{B}$  drift with respect to the electric field and L-shell based on the fitted results. **Errors in fitted equations in**

# Approach 2: Flow Angle Variation

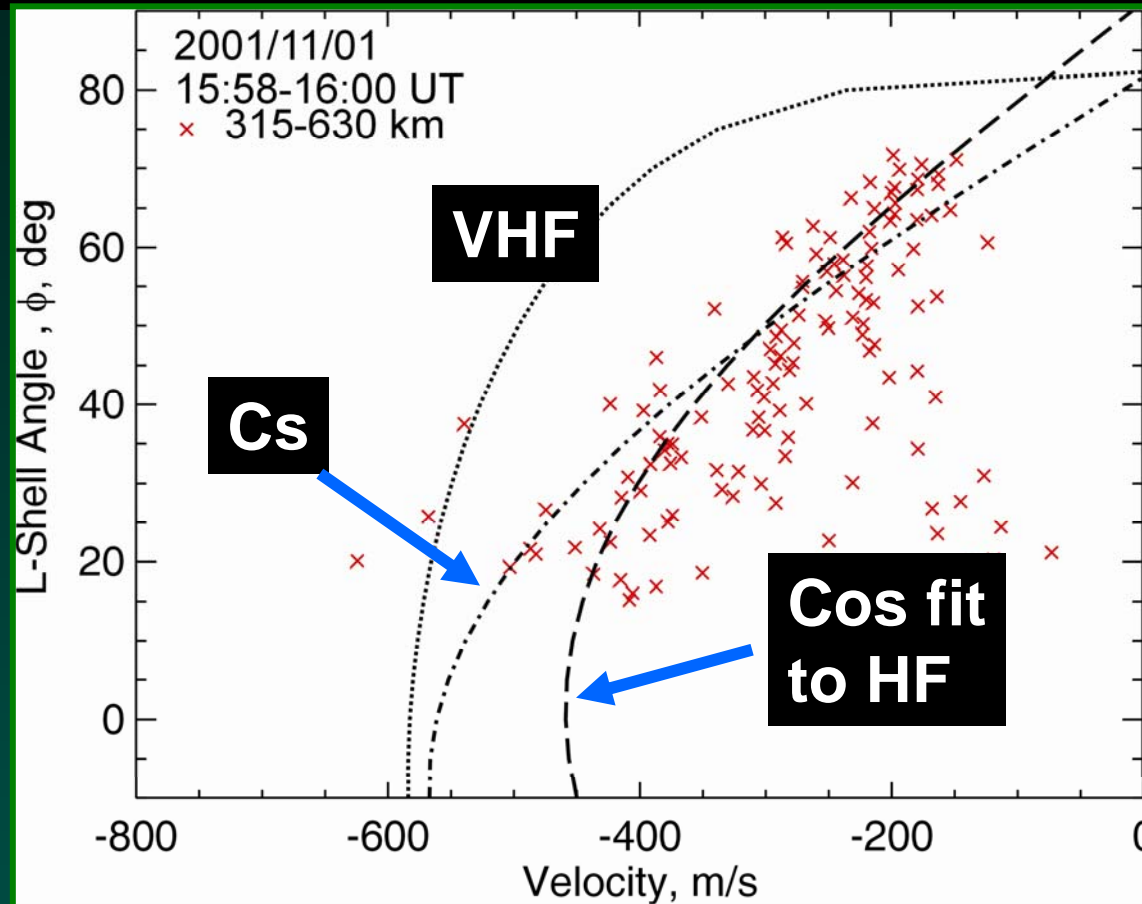
Each averaged velocity was associated with corresponding L-shell angle

The velocity vs L-shell angle variation was described in terms of a generic cosine function



- F-region peak velocity is higher than E-region peak velocity
- F-region (and generally E-region) peak is rotated from L-shell direction. The difference is 10 deg in this case

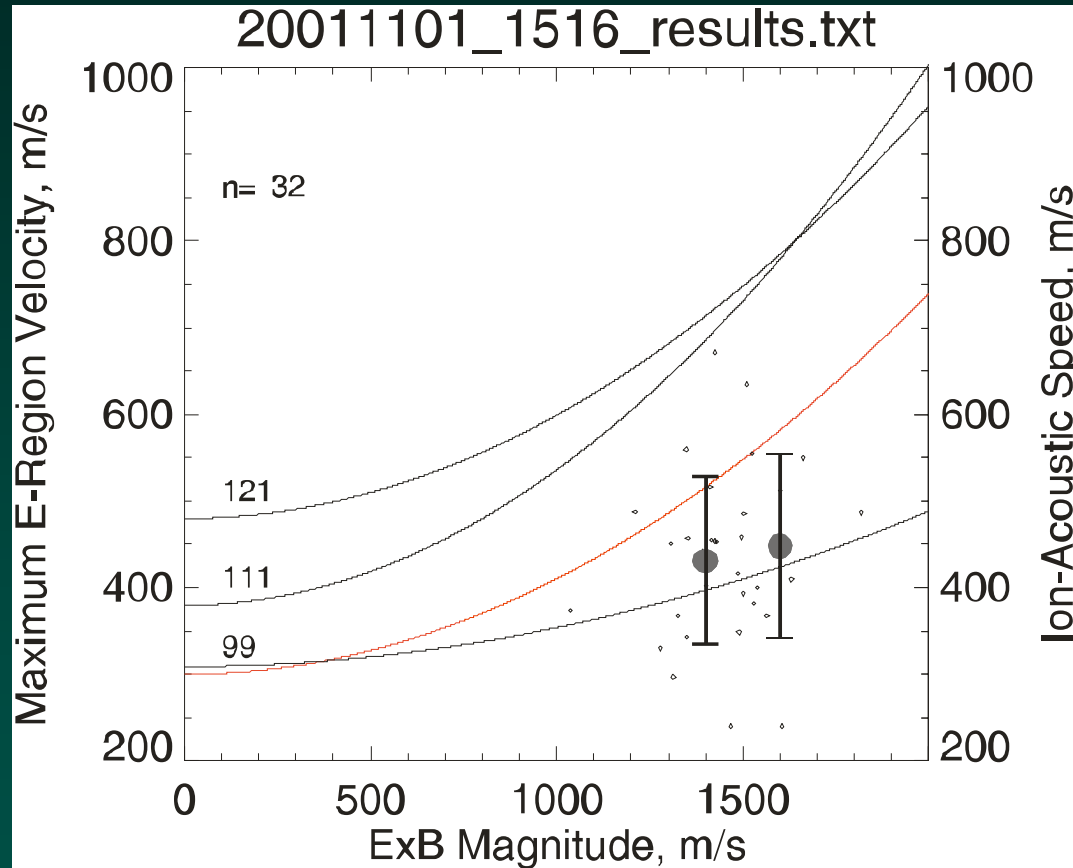
# HF vs VHF results and the $C_s$ hypothesis



- Strong disagreement with Nielsen et al. (2002) -VHF
- Better agreement with Bahcivan et al. (2005)-  $C_s$ , but peak velocity is typically below  $C_s$

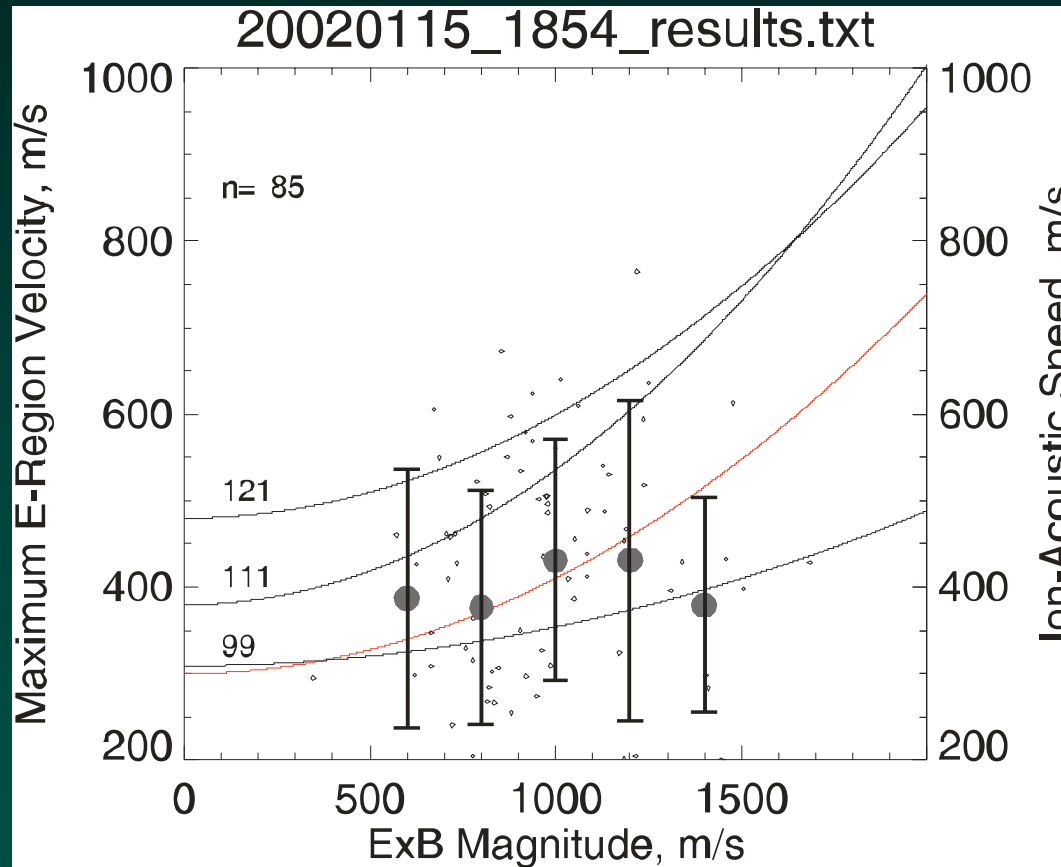


# Statistics: HF and the Cs hypothesis



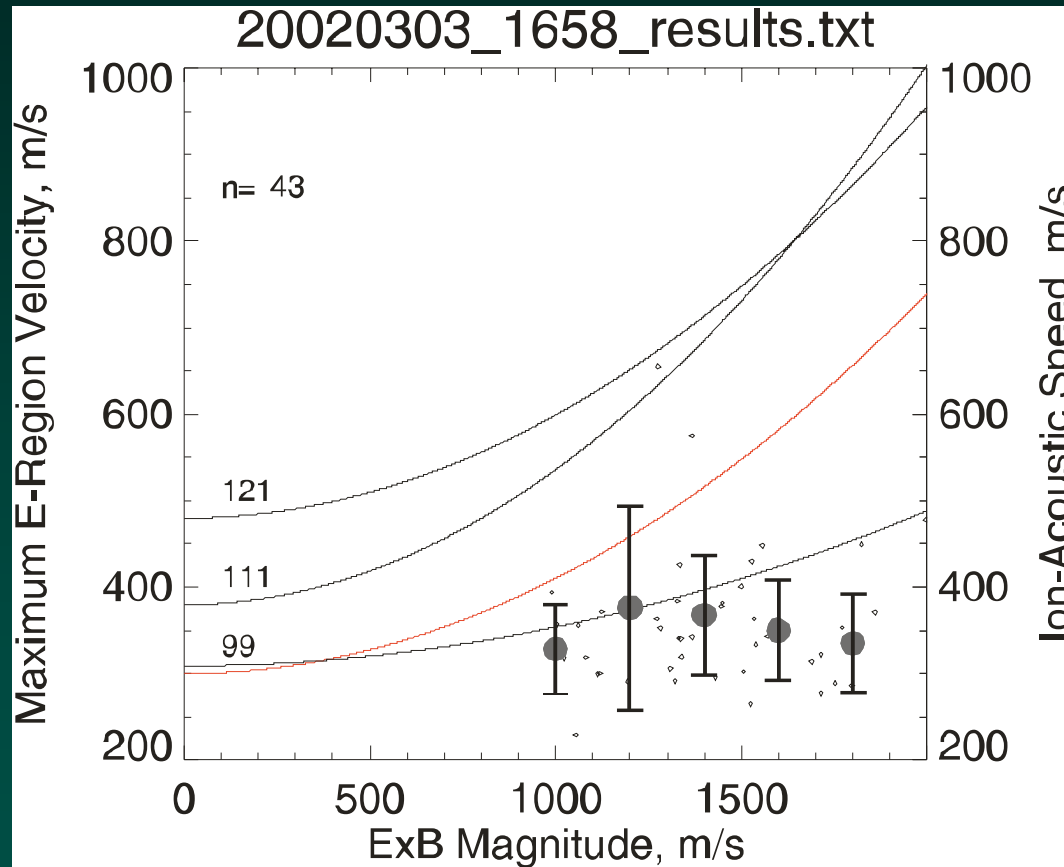
HF velocity agrees with Bahcivan et al. (2005), but only if all echoes are coming from below 100 km!

# Statistics: HF and the Cs hypothesis



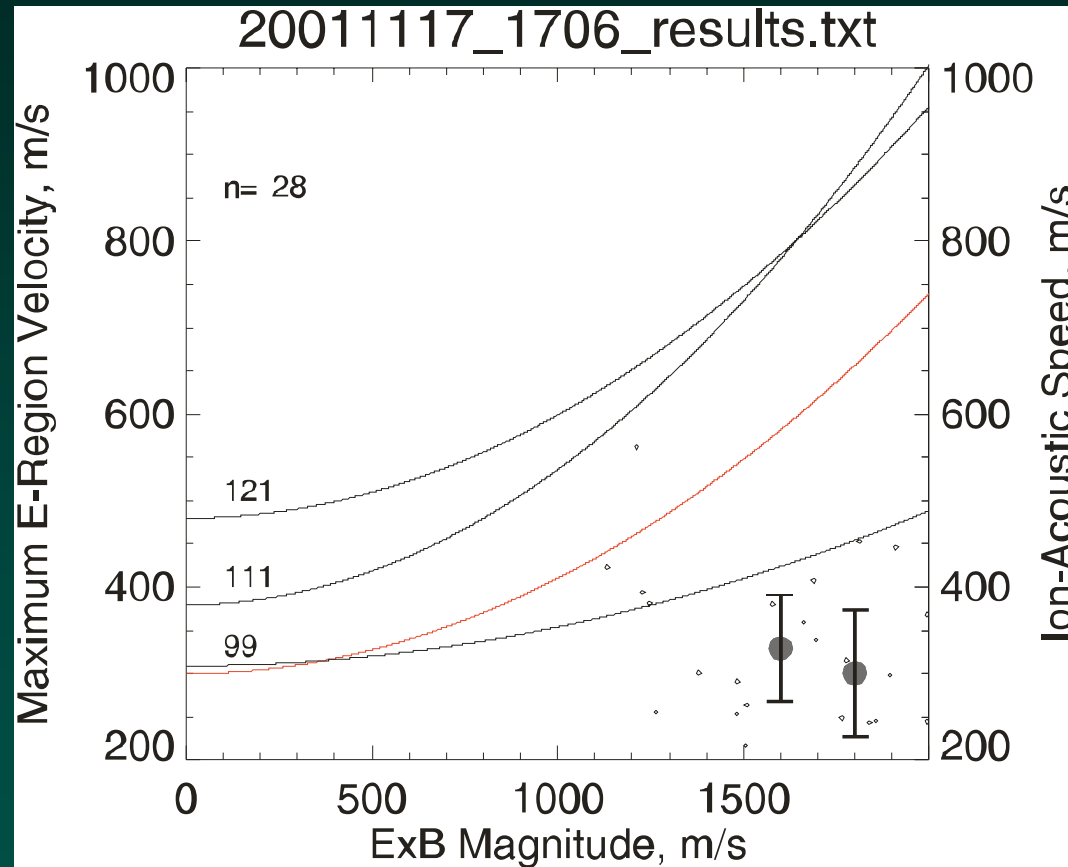
HF velocity agrees with Bahcivan et al. (2005), but only if all echoes are coming from below 100 km!

# Statistics: HF and the Cs hypothesis



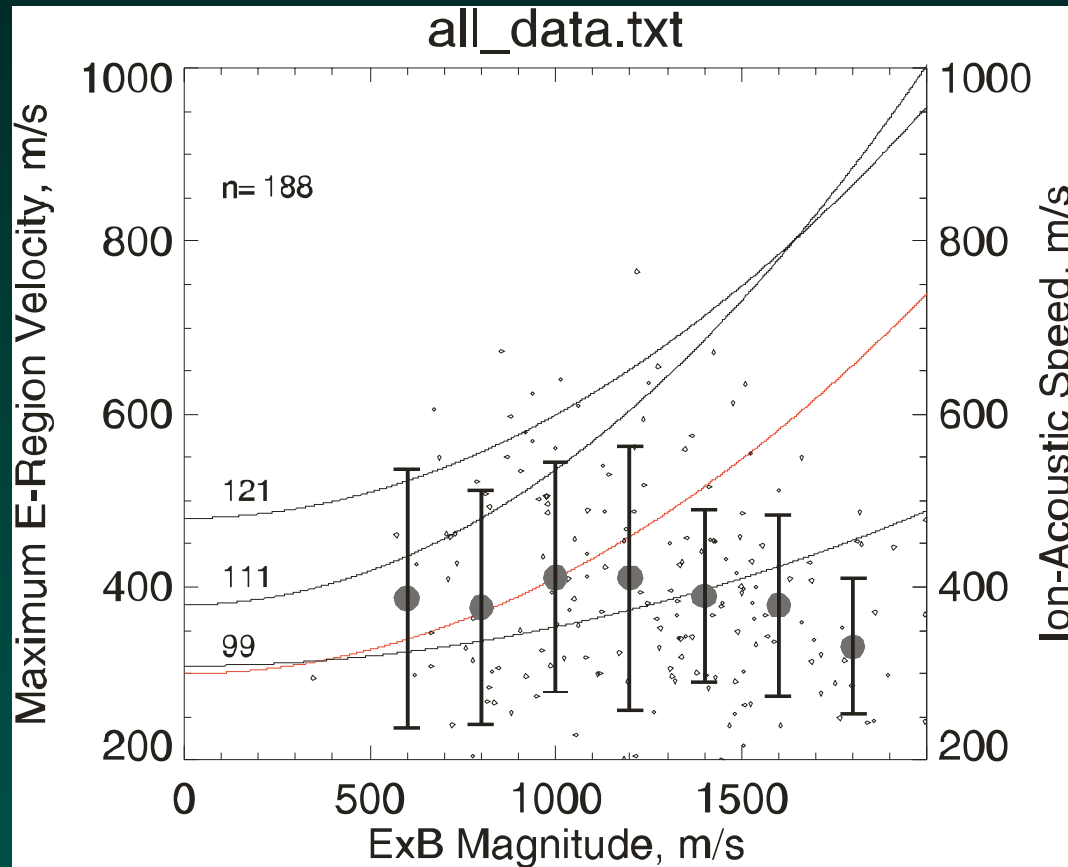
HF velocity agrees with Bahcivan et al. (2005), but only if all echoes are coming from below 100 km!

# Statistics: HF and the Cs hypothesis



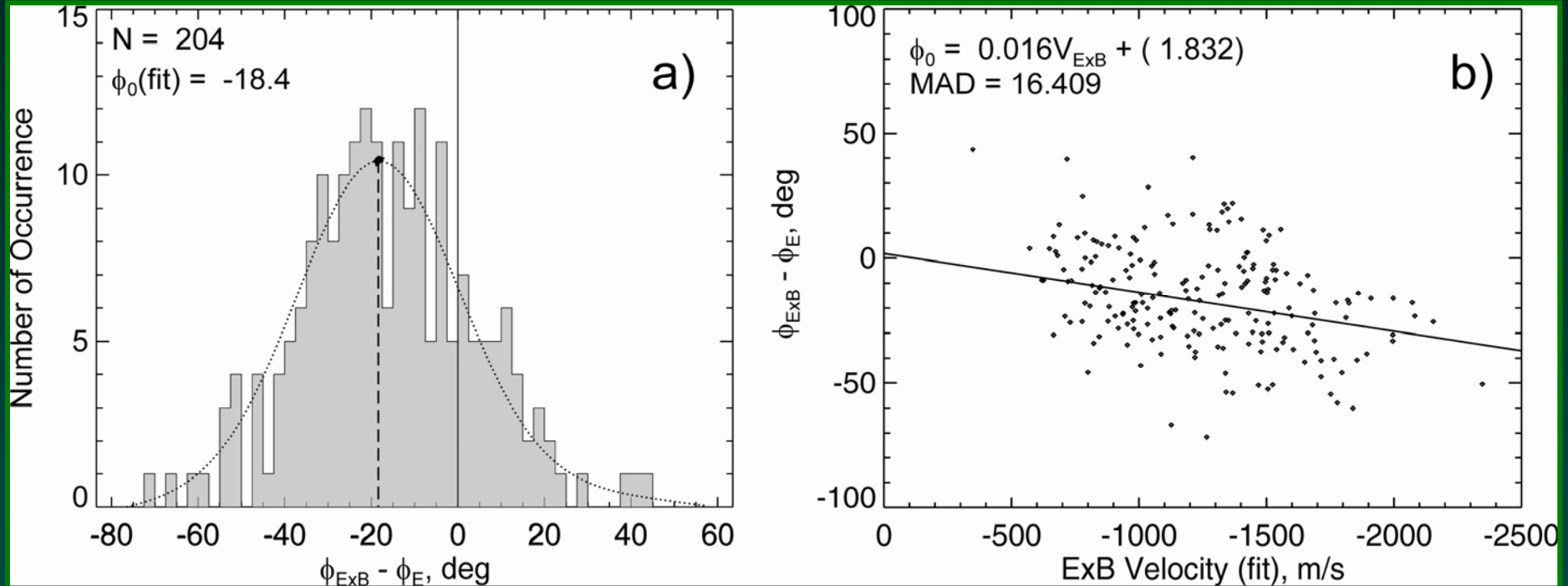
HF velocity is well below Cs

# Statistics: HF and the Cs hypothesis



HF velocity agrees with Bahcivan et al. (2005), but only if all echoes are coming from below 100 km!

# Velocity maximum and ExB direction



- A total of 184 scans from Stokkseyri for the events of 1 Nov 2001, 17 Nov 2001, 15 Jan 2002 and 3 Mar 2002 are considered
- Typical shift is  $\sim 20$  deg clockwise; it increases with ExB

# Velocity ratio ( $R=E/F$ ) for ALL events identified ( $> 60$ hours of common data)

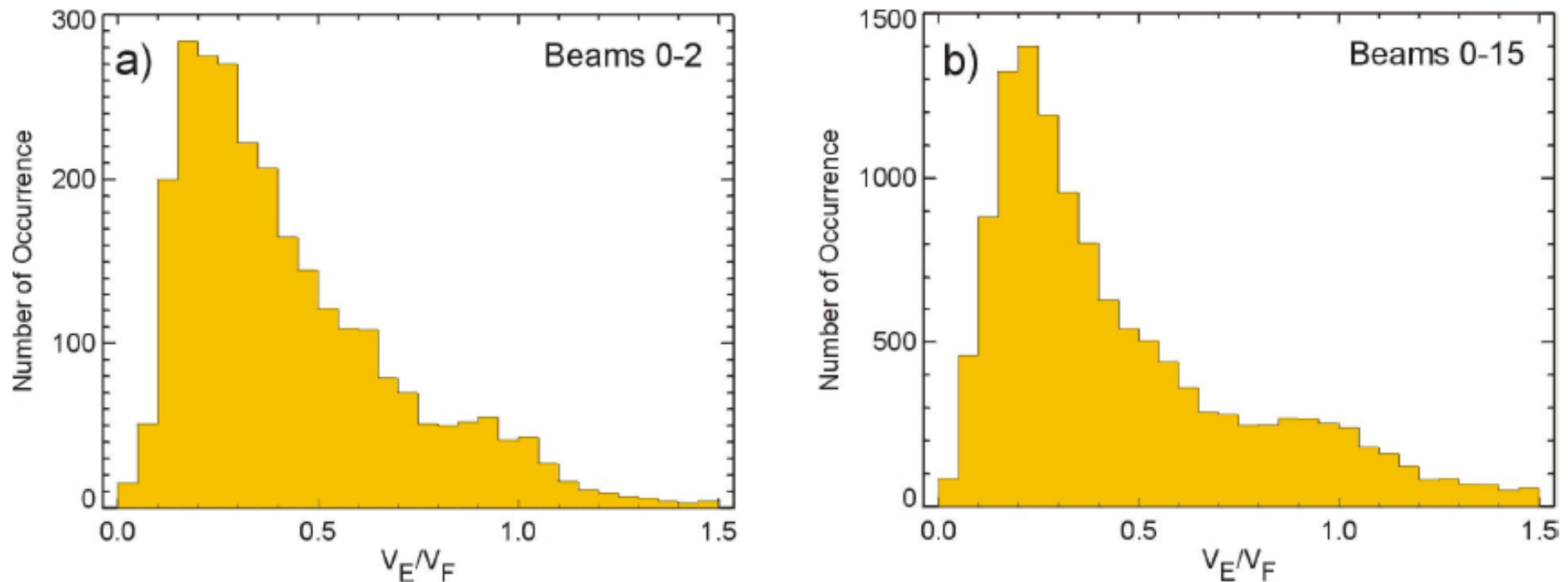


Figure 6.1: Histogram distribution for the velocity ratio  $R$  for the entire data set of 41 events: (a) in beams 0, 1 and 2 and (b) in all beams.

# Major Results of the Effort

1. Events were identified for which the E region velocity was significantly smaller than  $\mathbf{E} \times \mathbf{B}$ .  $\mathbf{E} \times \mathbf{B}$  magnitudes were of more than 600 – 800 m/s, typically above 1000 m/s. Observations covered a range of directions, from almost along  $\mathbf{E} \times \mathbf{B}$  to up to  $\sim 70^\circ - 80^\circ$  from  $\mathbf{E} \times \mathbf{B}$ .
2. Ratio  $\text{vel\_E\_region}/\text{vel\_F\_region} \sim 0.1-0.3$  for beams 0-2; weak dependence of the ratio upon  $\mathbf{E} \times \mathbf{B}$ .
3. Velocity variation with the flow angle can OFTEN be described reasonably by a cosine function. For these cases, the maximum velocity is well below  $\mathbf{E} \times \mathbf{B}$  and SOMETIMES close to  $C_s$  at the bottom of the electrojet. The maximum HF velocity is typically rotated away from the  $\mathbf{E} \times \mathbf{B}$  direction, towards E field, with a mean value of  $\sim 20^\circ$ .
4. Implication : Currently employed Map Potential technique for producing SuperDARN convection maps could underestimate the convection velocities at the equatorial edge of the SuperDARN combined zone of measurements and for PolarDARN radars at their short ranges.



The end

University of  
Saskatchewan

